Quantitative assessment of landslide susceptibility on a regional scale using geotechnical databases developed from GIS-based maps

Park D.W., Lee S.R.*, Nikhil N.V.*, Yoon S.* and Go G.H.
Department of Civil and Environmental Engineering, Korea Advanced Institute of Science and Technology (KAIST), Daejeon, KOREA
*srlee@kaist.ac.kr

Abstract

A practical application of a simple and economical solution to landslide susceptibility zonation using a geographic information system (GIS) was performed in Woomyeon Mountain, Seoul, Korea. The regional, physically based stability model of TRIGRS was used as the landslide susceptibility analysis. The accuracy of the model results depends primarily on a detailed knowledge of the study site and on the quality of the input parameters. However, the input data for the model is difficult to obtain because it not only requires test-based results but also spatial data.

An alternative application method for a physically based model in wide area using either GIS-based soil textures or geology maps is proposed for landslide susceptibility zonation. From a spatial database, the input data for the TRIGRS model including the material strength and hydraulic properties were extracted. The validation results exhibited satisfactory agreement between the calculated susceptibility zonation using different input layers and the existing landslide location on the landslide inventory. The use of these types of spatial maps linked with suggested geotechnical information enables reasonable estimation of the regions susceptible to landslides. Although the accuracy of the proposed model needs improvement, this approach is very useful for preliminary spatio-temporal assessments over large areas.

Keywords: Landslide, GIS, TRIGRS, soil texture, geology, database.

Introduction

In many countries, the yearly loss of property and life generated by landslides is larger than that from other natural hazards including earthquakes, floods and wind storms.[11] In total, more than 500,000 people died as a result of landslides in the 20th Century.[34] Korea is also prone to shallow landslides involving colluvium and these often mobilize into destructive debris flows.[17] Shallow landslides are typically 1-3 m deep and often occur at the boundaries between the colluvium and the underlying more solid parent rock.[36] In most areas of Korea, the thickness of the colluvium is generally less than 2 m due to the relatively shallow depth of the bedrock and hence shallow landslides are recurrent problem. Furthermore, the climate of Korea is typical of the Indian Ocean monsoon areas with significant seasonal precipitation.[16]

Thus, rainfall-triggered landslides cause extensive damage to people and to property. Due to the mountainous terrain with a shallow layer of colluvium and the associated weather conditions, landslides are hazard across most of Korea. Moreover, the socio-economic impact has become much higher than before as a result of the increased population levels in the hazardous zones. Therefore, landslide susceptibility assessment is a crucial issue in remedying this problem.

In order to understand when and where rainfall-induced landslides have occurred in mountainous regions and how the topographic, geotechnical and hydraulic parameters affect the initiation of landslides and how they might be used to predict the landslides, models that adopt both empirical and deterministic approaches have been used. There are four different approaches to the assessment of landslide hazards: (1) landslide inventory-based probabilistic model, (2) heuristic model that can be either a detailed geomorphological mapping[5] or an indirect qualitative map combination,[1,41] (3) statistical model that can be either a bivariate[35] or logistic regression[24] and (4) deterministic model.[6,11,44]

Among these models, the heuristic approach incurs subjectivity and is heavily dependent on the personal experience and knowledge of the experts involved.[46] In the statistical approach, these models cannot model nonlinear relationships and they also depend on the quantity and quality of accessible information and subjectivity of the map builder.[27] In contrast, the physically based and deterministic models are more objective and are frequently used for specific catchments because there are physical descriptions that can be used to inform the mathematical equations of the slope failure processes. Numerous models have developed e.g. SINMAP, SHETRAN, PROBSTAB, PISA, GEOtop-FS, and TRIGRS: this work focuses on the TRIGRS model. In

particular, simulations that use TRIGRS are very applicable to regions such as Korea which is prone to shallow rainfall-induced landslides.[2,3]

The Transient Rainfall Infiltration and Grid-based Regional Slope-stability (TRIGRS) model is written in FORTRAN code based on Iverson's[14] linearized solution of the Richards equation and the extension of that solution. The TRIGRS model, used for either saturated or unsaturated soils, can improve the effectiveness of the susceptibility analysis through considering the transient effects of varying rainfall on the conditions that affect the slope stability. The model has been used successfully around the world for quantitatively evaluating rainfall-triggered landslides.[6,10,16,27,29,30,36,37,39,44]

The TRIGRS model which is a deterministic model is based on calculating the safety factor. Deterministic models that provide the best quantitative information on landslides are more reasonable approaches for land susceptibility mapping.[40] However, applying the models at a regional scale incurs difficulties in the availability and validation of data in large spatial data sets as input parameters.[34] Therefore, an alternative must be determined in order to resolve these problems. The TRIGRS model includes various input data such as time-varying rainfall, topographic characteristics, soil depth, material strength and hydraulic properties.[2,3]

However, collecting these input data from field investigations or laboratory tests is difficult particularly on a regional scale. Moreover, almost all natural soils are highly variable in their properties and are rarely homogeneous. For these reasons, an improvement or alternative to obtaining the input parameters for wide areas is required in the prediction of shallow landslides. Using the characteristic factors related to landslide initiation such as the soil texture, geology, topographic type, soil drainage, soil type and land use as an indirect method can be an alternative method because these input data are readily available for the whole of Korea from the relevant national research institutes.[11]

Soil texture is a term commonly used to designate the distribution proportion of the different sizes of soil particles.[4] That is, it describes the relative proportion of the different sizes of individual mineral particles, sand, silt and clay, without considering the organic matter. Among the diverse soil characteristics, texture is a key factor that constols the soil behavior. For this reason, the first system used by geotechnical engineers classified soil by grain size or soil texture.[12]

The soil texture influences the movement of water and air through voids as well as the water content of the soil. In soils that are predominantly sandy, the hydraulic conductivity is high and the water content is low because sand has a small surface area and is more prone to water repellence. In contrast, clay soils have slow water transmission capability and high water retention. These types of soil restrict not only the water and air movement but also the water entry into the soil compared with sandy soils.

The soil texture also affects the soil strength. The soil strength of aggregated soils increases as the clay content increases; therefore, single grain or poorly aggregated soils such as sands, loamy sands and sandy loams usually have the weakest soil strengths unless they are cemented or compacted. The individual particles of single grain soils are prone to rearrangement but these soils are easily influenced by compaction resulting in the formation of hard pans. This often occurs in Korea's Coastal Plain region that primarily consists of sandy soils.

The USDA system for determining the texture classification differs significantly from the Unified Soil Classification System (USCS) and the American Association of State Highway and Transportation Officials (AASHTO) system that are traditionally used by worldwide engineers. The first significant difference is the threshold between the particle sizes among the three systems. The second significant difference is that the USDA classification system depends entirely on particle size: the Unified and AASHTO classification systems rely on both particle sizes and other test results such as the Atterberg limits. However, in Korea, a spatial database that combines the grain size and Atterberg limits does not exist yet.

Comparable with the soil texture, the surficial lithology also has a significant function in soil characteristics. In a natural slope, soil layers are commonly called unconsolidated soil and include the rock mass and rock type.[43] Soil is defined as the sediments or other accumulations of mineral particles formed by the physical or chemical disintegration of primarily rock and the air, water, organic matter and other substances that may be included. Thus, the physical characteristics of the upper soil differ according to the geological conditions of the bedrock.[13]

The influence of the surficial lithological characteristics on the hydraulic properties has remained obscure. Regarding permeability, the constant of proportionality is represented using the geological properties of the soil medium. For the medium, the properties that determine the flow rate are related to the particle structure and geological origins such as the mineralogy, weathering and sedimentary environment. High values of saturated hydraulic conductivity were present in the lithology with a sandy matrix in regions of felsic granitoids or granite gneisses while low values were typically found in the lithology derived from sedimentary rocks.

All geological materials have an ability to resist failure under stresses and this is referred to as strength. The shear strength of each lithology is a function of lithological characteristics (clay content, clay mineralogy etc.) and other engineering properties (natural water content, specific gravity, void ratio, absorption, adsorption, Atterberg limits etc.). If the grains are densely packed, the cementing mineral is strong (e.g. quartz) and there are few pore spaces, the lithology type is extremely strong. The soils have a wide variety of strengths depending on their lithology varying from strong or medium strong rocks e.g. sericite metasandstone, limestone, greywacke and sericite schist through to weak rocks e.g. meta-siltstone, clayey and silty shale and phyllite.

The primary objective of this paper is to discuss the application of different spatial databases as input parameters to manage the physically based model in a large area. TRIGRS model simulations for the study area according to different scenarios are conducted in order to estimate the applicability of the physical model. In order to obtain a quantitative comparison of the models using both geotechnical investigation data and open source databases such as soil texture and geology, a landslide inventory map of the case study was developed. Furthermore, other landslide susceptibility models that are used in Korea are cited for quantitative validation. Finally, the limitations of the current application are addressed and potential solutions and guidelines for future studies are proposed.

Case Study

Study area: The study area was Woomyeon Mountain which is located in the Seocho district of Seoul, South Korea (Fig. 1). It is located at 37°27′00″N - 37°28′55″N latitude and 126°59′02″E - 127°01′41″E longitude. The elevation of Woomyeon Mountain is 293 m above sea level. The study area, which is encircled by buildings and roads, amounts to 5,104,162 m^2 and is predominantly covered by forest with mostly oak trees.

The geology of the Woomyeon Mountain region primarily consists of gneiss and granite. The banded biotite gneiss was moderately weathered and has stripes called gneissic banding which develop under conditions of high temperature and pressure. Due to the gneissic banding, it is clear that the study area has been exposed to extreme shearing.

The soil profile can be divided into three layers[19]: a colluvium layer extending to a maximum depth of 3.0 m from the ground level, a transition zone composed of primarily a clay layer (thickness: 0.2 m to 0.5 m below colluvium layer) and a subsoil of stiff weathered bedrock followed by another clay layer.

Landslide event: From July 26 to July 27, 2011, a heavy rainfall (470 mm in two days) occurred in Seoul that was approximately 20% of the total annual rainfall for the region. During this precipitation event, 147 catastrophic landslides occurred on Woomyeon Mountain. Most landslides were accompanied by debris flows and the mixtures of debris flowed down the roads into the surrounding communities. Sixteen people were killed and ten buildings were damaged by these debris flows which led to economic losses of approximately US$15 million. During the storm, the shallow landslides on the steep mountainous terrain were primarily triggered by the heavy rainfall that increased the pore pressure of the soil in the near-subsurface with an attendant decrease in the soil's shear strength. Under these conditions, the precipitation-induced landslides caused translational mass movements that occurred suddenly. Fig. 2 depicts the locations of the damaged districts (landslide scarps, debris flow area and inundated buildings) after the disaster.

Creating a landslide inventory: Accurate mapping of landslides is very important for landslide susceptibility analyse. Although mapping of landslides appears to be an objectiv.[42] van Westen et al[42] examined the agreement of different landslide inventory maps through comparing the independent mappings of three different teams of geomorphologists for the same area in the Alpago area in Italy. As a result, two of the three landslide inventory maps were similar but one map differed considerably. This indicates that landslide inventory mapping can vary when conducted by different teams because direct landslide susceptibility mapping is a subjective task that relies on the expertise, experience, assessment and opinions of the researcher.

In addition, collecting data such as satellite images, aerial photographs and field investigations to identify landslides are essential for accurate landslide inventories. Many studies have illustrated the application of remote-sensing data for landslide.[9,28,33,45] In this study, aerial photographs with a resolution of 25 cm and satellite images with a resolution of 1 m taken before and after the landslide event were used to detect the precise landslide locations. After digitizing the estimated landslide points, a temporary landslide inventory map was compared with the field investigation map registered in an official archive of disaster survey reports and publications for the Seoul government by the Korean Society of Civil Engineers.[20] Fig. 3(a) presents the landslide locations and this image is suitable for identifying and mapping the landslides in fig. 2(a). The landslide map identified 147 individual landslides with a landslide density of 29 landslides/km^2. Most landslides transformed into translated debris flows as plotted in fig. 2(a).

Spatial database

Many important parameters are involved in the TRIGRS model e.g. the topographic factors and soil thickness, as well as the strength and hydraulic parameters of the soil. In order to apply a distributed model, the input parameters must be constructed into a spatial database in a GIS platform. The aerial photographic, satellite image, precipitation, topographic, geotechnical investigation, soil texture and geological data in the study area were collected as described in table 1. These data are available for all of Korea in either digital maps or paper maps. Then, these data were constructed into a spatial database for the application of the TRIGRS model. The ArcGIS was used to create grids with 10 m cells and to quantify the aforementioned information for each cell of the Digital Elevation Model (DEM).

A key assumption of the approach used in this study is regarding the hydraulic parameters including the hydraulic saturated conductivity (K_s), diffusivity (D_0) and steady infiltration rate (I_z). The values of D_0 and I_z were not well defined because they had wide ranges according to the complex properties of the soil (e.g. voids, fine content and soil density). Liu and Wu[27] proposed that the D_0 value could be assumed to be 200 times that of the K_s and I_z is 0.01 times that of K_s, based on the literature.

In the simulations conducted in this study, a uniform soil depth of 2 m was used due to the similar value of the soil depth in various reports[19] and the presence of shallow landslides mostly between 1 and 3 m in Korea. The initial ground water table was set at the same depth of soil thickness due to a lack of heavy antecedent rainfall before the event and the hot, dry conditions during the summer of this event.[16]

For the rainfall, the rainfall intensity database was obtained from weather stations operated by the Korea Meteorological Administration. There are three meteorological monitoring stations (Namhyun, Seocho and Gwacheon) near Woomyeon Mountain. The climate in the study area is characterized by an average annual rainfall of 1400-1500 mm with the highest rainfall in July and the lowest in January. However, the climatic conditions in July 2011 differed significantly to the average. During July alone, Woomyeon Mountain received approximately 55% of its total annual precipitation of 2039 mm. The hourly maximum rainfall was 114 mm/hour (07:44-08:44 on 27 July 2011) which was 120 years of rainfall recurrence interval at Namhyun Station. Fig. 4 presents part of the rainfall input layers (hourly rainfall intensity from 08:00 to 09:00 on 27 July 2011) using this analysis.

Geotechnical investigation database: All available data were obtained from the geotechnical engineering investigation of the landslide hazard restoration work conducted by the National Forestry Cooperative Federation[32], Korean Society of Civil Engineers[20] and Korean Geotechnical Society[19]. After the landslides occurred on July 27th, a total of 58 geotechnical investigation boreholes were drilled in order to investigate the ground condition, hydrologic and geological information. Among these, 19 soil samples were collected from 13 sites which were evenly distributed across Woomyeon Mountain and various geotechnical field or laboratory tests were conducted in order to understand the soil characteristics more accurately.

The locations of the investigation boreholes and profiles are depicted in fig. 5. The study area was divided into five zones based on the catchment and engineering properties. The input values and parameter units according to the property zones are listed in table 2.

Soil texture database: Korea Forest Service provides forest soil maps including soil textures for all of Korea. These maps with a scale of 1:25,000 were developed from field investigations over a long period of time and are being updated constantly. The types of soil included in these texture maps by Korea Forest Service were sandy loam (SL), loam (L), silt loam (SiL), silty clay loam (SiCL), sandy clay loam (SCL), silty clay (SiCL), clay loam (CL), clay (C), loamy sand (LS) and sand (S) based on the soil separates system defined by the USDA. The soil texture of the study area consists primarily of sandy loam and silt loam as shown in fig. 6.

There is literature available regarding the numerically suggested values of the hydraulic properties and material strengths. The infiltration characteristics such as the saturated hydraulic conductivity and unsaturated properties were proposed by Clapp and Hornberger.[7] They tested 1446 soil samples and derived the representative values according to the soil classes. In terms of soil strength, the National Disaster Management Institute (NDMI) proposed the unit weight, cohesion and internal friction angles as the recommended values of soil in Korea.[31]

The relationship between the landslide and soil texture has been established in the literature. The landslide occurrence probability is higher in gravelly loam, rocky sandy loam and rocky loam and is lower in loam and sandy loam. The relationships are primarily attributed to the soil grain size. During heavy rain, if the grain size is greater, water can flow quickly through the soil due to the higher porosity[12,21] which makes the slope more susceptible to landslides.

Geology database: A geological map of the study area with a scale of 1:50,000 was developed by the Korea Institute of Geoscience and Mineral resources (KIGAM) as depicted in fig. 7. The categories of rock types that form the basis for the

soil are based on the geological and mineralogical data. The hierarchical categories based on the KIGAM maps include igneous, sedimentary and metamorphic geology.

Jun et al[15] estimated the average hydraulic properties and proposed simple equations for estimating permeability according to the geologic conditions. The soil tests were performed on the specimens obtained from approximately 1,150 sites including landslide and non-landslides areas in natural terrains for the past 10 years in Korea. For the material strength, Kim[18] conducted tests as objects of the soil layer of natural slopes in landslides areas. In that study, the different soil specimens that had various lithological types were tested in a multiple-reversal direct shear device in order to measure the shearing resistance of the gneiss, granite and sediment soils. Those results are reliable because the geology was classified using a geology map from KIGAM in the research. The geotechnical data which was obtained from the studies of Jun et al[15] and Kim[18] have been assigned to each cell on the basis of the previously defined three primary lithological units which are summarized in tables 4(a) and 4(b).

In the relationship between landslides and lithology, landslides are frequently observed in granite gneiss and leucocratic gneiss areas but are unusual in quartz mica schist and biotite gneiss areas.[25]

Description of the TRIGRS model

TRIGRS models the rainfall infiltration that results from storms that have durations ranging from a few hours to a few days. To do so, it uses the analytical solutions of partial differential equations that represent one-dimensional vertical flows in isotropic homogeneous materials for either saturated or unsaturated soil conditions (Fig. 8). This process combines the theoretical bases of the models for infiltration and subsurface flows of storm water, routing of runoff and slope stability in order to calculate the effects of the rainfall on the analysis of the stability over large areas. It is possible to analyze complex storm sequences over complex geomorphological terrains because the infiltration, hydraulic properties and slope stability input parameters are allowed to vary over the grid area. The safety factor of each pixel in the area is calculated analytically. The following provides a brief description of the infiltration and slope stability model used by TRIGRS to represent these processes.

Infiltration model: The infiltration models in TRIGRS for initial wet conditions are based on Iverson's[14] linearized solution of the Richards equation and on the extensions by Baum et al[2,3] to that solution. Only a short description is presented here since many authors have used and described the TRIGRS model in detail over the past decade. The generalized solution of pore pressure is given as follows:

$$\psi(Z,t) = (Z-d)\beta$$

$$+2\sum_{n=1}^{N}\frac{I_{nZ}}{K_S}H(t-t_n)[D_1(t-t_n)]^{\frac{1}{2}}\sum_{m=1}^{\infty}\left\{ierfc\left[\frac{(2m-1)d_{LZ}-(d_{LZ}-Z)}{2[D_1(t-t_n)]^{\frac{1}{2}}}\right]+ierfc\left[\frac{(2m-1)d_{LZ}+(d_{LZ}-Z)}{2[D_1(t-t_n)]^{\frac{1}{2}}}\right]\right\}-$$

$$+2\sum_{n=1}^{N}\frac{I_{nZ}}{K_S}H(t-t_{n+1})[D_1(t-t_{n+1})]^{\frac{1}{2}}\sum_{m=1}^{\infty}\left\{ierfc\left[\frac{(2m-1)d_{LZ}-(d_{LZ}-Z)}{2[D_1(t-t_{n+1})]^{\frac{1}{2}}}\right]+ierfc\left[\frac{(2m-1)d_{LZ}+(d_{LZ}-Z)}{2[D_1(t-t_{n+1})]^{\frac{1}{2}}}\right]\right\} \quad (1)$$

where ψ is the ground-water pressure head, d is the steady-state depth of the water table measured in the vertical direction and $Z = z / \cos\delta$. Here, Z is the vertical coordinate direction (positive downward) and depth below the ground surface, z is the slope-normal coordinate direction (also positive downward) and δ is the slope angle. d_{LZ} is the depth of the impermeable basal boundary measured in the vertical direction and $\beta = \cos^2\delta - (I_{ZLT} / K_S)$, in which K_s is the saturated hydraulic conductivity in the Z direction, I_{ZLT} is the steady (initial) surface flux and I_{nZ} is the surface flux of a given intensity for the n^{th} time interval.

$$D_1 = D_0 / \cos^2\delta$$

where D_0 is the saturated hydraulic diffusivity ($D_0 = K_S / S_S$ where K_S is the saturated hydraulic conductivity and S_S is the specific storage). N is the total number of time intervals; m is the index of the infinite series displaying odd term in the complementary error function. H (t - t_n) is the Heaviside step function and t_n is the time at the n^{th} time interval in the rainfall infiltration sequence. The function erfc(η) is the complementary error function where ierfc(η) = $(1/\sqrt{\pi})$ exp($-\eta^2$) - η erfc(η).

Slope stability model: The model of the slope stability in ∂d TRIGRS uses an infinite slope stability analysis which assumes that the slope is infinitely long and planar failure surface. It is characterized by the ratio of resisting friction to gravitationally induced downslope driving stress. In this scheme, FS < 1 denotes unstable conditions and the depth Z, where FS first drops below 1, will be the depth of the landslide initiation. The equation for calculating the safety factor of the slope incorporating eq. (1) into the classic an infinite slope model is given as follows:

$$FS(Z,t) = \frac{\tan\phi'}{\tan\delta} + \frac{c' - \psi(Z,t)\gamma_w\tan\phi'}{\gamma_S Z\sin\delta\cos\delta} \quad (2)$$

where c' is the soil cohesion for effective stress, ϕ' is the soil friction angle for effective stress, γ_w is the unit weight of

groundwater and γ_s is the unit weight of the soil. Further theoretical details of the model have been fully described in the TRIGRS open file reports.[2,3]

Results and Discussion

A key objective of this research was to evaluate the spatiotemporal predictability of landslide events in Woomyeon Mountain using the TRIGRS model for different input parameter databases of geotechnical investigation, soil texture and geology. Fig. 9(a) and 9(b) present the resulting safety factor over the study area for the application of geotechnical investigation database. For a severe storm, the resultant safety factor exhibits different levels of landslide susceptibility according to the property zones (Fig. 5). However, a landslide did not occur in zone 3 due to the high value of strength and small hydraulic conductivity. The areas with safety factors of less than 1.0 were predominantly located in regions of high permeability and low shear strength along the steep mountain slopes.

Fig. 10 presents the spatial distributions of the safety factors for the two input databases: soil texture [Fig. 10(a)] and geology [Fig. 10(b)]. For each database, the TRIGRS model reasonably simulated the spatial probability of landslides as in the geotechnical investigation database scenario.

For the soil texture database based on the soil texture map, the areas characterized with a safety factor less of than 1.0 were sizeable as seen in fig. 10(a). This is because sandy loam comprises the vast majority of the study area and it has a smaller value of soil cohesion than silt loam. This trend of the region with a small cohesion being more susceptible appeared in the application results of the geology database as depicted in fig. 10(b). In the deterministic slope stability analysis, the safety factors are more sensitive to the soil cohesion than the internal friction angle for typical ranges.[38] Furthermore, the soil cohesion has greater spatial variability than the frictional parameter.[8] Therefore, among the landslide susceptibility parameters, the spatial variation in the soil cohesion most significantly influences the safety factor calculations.

Along the boundary between the housing sites and mountainous areas, unstable regions were predicted because the DEM does not consider the number of retaining walls and reinforced excavated slopes. Nevertheless, the performance of the TRIGRS model for prediction which was evaluated through a landslide inventory is considered appropriate as shown through figs. 9 and 10.

For the quantitative validation of the landslide susceptibility mapping for each scenario, the cumulative frequency diagram shown in fig. 11 and table 5 were applied. In this scheme, the validation was performed through comparing the known landslide location data from the inventory with the landslide susceptibility simulation results for the three types of spatial databases. In order to compare the relative accuracy for each application, the calculated safety factor values of all cells in the study area were ranked in descending order and this is known as the landslide susceptibility index rank.[26]

Then, the ordered cell values were divided into 20 classes with 5% intervals. The cumulative percentage of the landslide occurrence within these divided classes was marked. It is natural for classes with a high landslide susceptibility rank to contain more landslides if the model is valid. Ideally, the slope of the curve should decrease consistently.

For example, for the model using the input properties from the geotechnical investigation database, the 80 to 100% (20%) class of the study area where the landslide susceptibility index had a higher rank included 99.3% of all landslides. That is, 99.3% of the actual landslides were correctly localized within 20% of the predicted susceptible area. In addition, it occupies 62.8% of the study area using the soil texture database and 75.2% of the study area using the geology database as summarized in table 5. Among the three estimation procedures considered, the geotechnical investigation database is used as the input parameters demonstrated the best performance in the every class. Although the simulation performance using the geology database was similar to that using the soil texture map, the former was better than the latter in the 55~95% classes.

The success rate of the previous research results that used various statistical models in Korea[22,23,26] has been cited in comparison with the conventional statistical approaches: the frequency ratio, weight-of-evidence, likelihood ratio, logistic regression and neural network models were used to develop a susceptibility map for Korea. As a result, for the 80 to 100% class (20% of the high ranked susceptible areas in their simulation), the success rate for these models was reported to be 64% for the frequency ratio, 54% for the weight-of-evidence, 50.8% for the likelihood ratio, 49% for the logistic regression and 39.1% for the neural network. The performance of the physically based model using the indirect material strengths and hydraulic properties exhibited better results from a quantitative perspective, despite the small database (i.e. 62.8% of the soil texture map and 75.2% of the geology map).

As a general conclusion, the slope stability models can be applied successfully at a regional scale when the quality of the input data is good and is appropriately constructed and modeled. In the same context, recent studies have demonstrated that the best approach for landslide spatial prediction is the application of deterministic models

combined with transient or steady state infiltration models for hill slope hydrology.[34]

For a quantitative comparison, the areas under the curve in fig. 11 were recalculated as a total area which equals 1 for perfect prediction. The rate explains how well the model and input factors predict shallow landslides. Thus, the area can be used to assess the prediction accuracy. The result with the geotechnical investigation data demonstrated that the area ratio was 0.9574; thus, it is considered that the prediction accuracy is 95.74%. The areas under the curves of soil texture data and geology data results were 0.8209 and 0.8471 respectively which indicate 82.09% and 84.71%.

Conclusion

Deterministic models provide the best quantitative results for landslide hazard detection that can be used directly in the design of engineering works and in the quantification of risk. However, these models need a large amount of detailed input data derived from field investigations and laboratory tests as well as the construction of continuously distributed data for the information.

This paper proposed a deterministic approach using the suggested soil properties as input data from GIS-based soil texture and geology databases in order to assess rainfall-induced shallow landslides in a mountainous region in Seoul, Korea. The simulations were conducted at two levels: (i) constructing the GIS-based spatial database for TRIGRS input parameters and landslide inventory and (ii) analyzing a case study for 147 shallow landslides that occurred during an intense rainfall event in July 2011 considering the various input conditions. The suitability of these methods was tested through comparison with the conventional method of direct utilization from field investigations and laboratory tests which have previously been proven to be reliable in identifying anomalies in susceptibility analyses.

The validation results demonstrated that the performance of the simulation results with well-measured geotechnical data is a prediction accuracy of 95.74% in the success rate method, and the result using the geology data has a better predication accuracy of 2.62% (84.71-82.09%), higher than that using the soil texture database. The model simulations resulted in reasonable estimates of the mountain hazards based on a deterministic approach at a regional scale. It is noteworthy that the proposed approach is useful when field investigation and laboratory test results are not available for the entire region.

Although the indirect approach has many advantages, there are limitations that can reduce the model accuracy and continual research is required in the following areas:

(1) A number of verifications with other case studies that have different regions, data and scales are necessary. As a result of the small area and the 1:50,000 scale geology map that was used in this study, there are a number of lithology types within the study area and hence a wider study area is needed.

(2) The proposed values for the soil material in this study should be verified and corrected continuously in order to improve the model accuracy. It is very important to note that the soil texture alone does not provide sufficient information about soils. Thus, understanding and predicting the soil behavior and suitability are required.

(3) In order for the method to be applied, the landslide-related data in spatial form is essential. In Korea, the landslide-related spatial data for the topography, soil and geology are available either as a digital map or a paper map.

Acknowledgement

This study was supported by the National Research Foundation of Korea under the Ministry of Education, Science, Technology (under grant No. 2013M3A2A1054838) and Korean Ministry of Land, Transport and Maritime Affairs (MLTM) as part of the U-City Master and Doctor Course Grant Program.

References

1. Barredo J., Benavides A., Hervas J. and van Westen C.J., Comparing heuristic landslide hazard assessment techniques using GIS in the Tirajana basin, Gran Canaria Island, Spain, *International Journal of Applied Earth Observation and Geoinformation*, **2,** 9–23 **(2000)**

2. Baum R.L., Savage W.Z. and Godt J.W., TRIGRS – a FORTRAN program for transient rainfall infiltration and grid-based regional slope stability analysis, US Geological Survey Open-File Report 2002-424, 38 **(2002)**

3. Baum R.L., Savage W.Z. and Godt J.W., TRIGRS – A FORTRAN program for transient rainfall infiltration and grid-based regional slope stability analysis, version 2.0, US Geological Sur-vey Open-File Report 2008-1159, 75 **(2008)**

4. Brown R.B., Soil Texture, Institute of Food and Agricultural Sciences, University of Florida, Fact Sheet SL-29 **(2003)**

5. Castellanos E. A. and van Westen C.J., Qualitative landslide susceptibility assessment by multicriteria analysis, a case study from San Antonio del Sur, Guantánamo, Cuba, *Geomorphology*, **94,** 453-466 **(2008)**

6. Chen C.Y., Chen T.C., Yu F.C. and Lin S.C., Analysis of time-varying rainfall infiltration induced landslide, *Eng. Geol*., **48(4),** 466-479 **(2005)**

7. Clapp R.B. and Hornberger G.M., Empirical Equations for Some Soil Hydraulic Properties, *Water Resources Research*, **14(4),** 601-604 **(1978)**

8. Crosta P.B. and Frattini P., Preface Rainfall-induced landslides and debris flows, *Hydrol. Process*, **25,** 473-477 **(2008)**

9. Dai F.C., Lee C.F. and Wang S.J., Characterization of rainfall-induced landslides, *International Journal of Remote Sensing*, **24(23),** 4817-4834 **(2003)**

10. Godt J.W., Baum R.B., Savage W.Z., Salciarini D., Schulz W.H. and Harp E.L., Transient deterministic shallow landslide modeling: Requirements for susceptibility and hazard assessments in a GIS framework, *Eng. Geol*., **102,** 214–226 **(2008)**

11. Guzzetti F., Carrarra A., Cardinali M. and Reichenbach P., Landslide hazard evaluation: a review of current techniques and their application in a multi-scale study, Central Italy, *Geomorphology*, **31(1-4),** 181–216 **(1999)**

12. Holtz R.D. and Kovacs W.D., An Introduction to geotechnical engineering, Prentice Hall **(1981)**

13. Hutchinson J.N., Morphological and geotechnical parameters of landslides in relation to geology and hydrology, In Landslide Proc. 5th Int. Symp. on Landslide, **1,** 3-35 **(1988)**

14. Iverson R.M., Landslide triggering by rain infiltration, *Water Resour. Res.*, **36,** 1897–1910 **(2000)**

15. Jun D.C., Song Y.S. and Han S.I., Proposal of Models to Estimate the Coefficient of Permeability of Soils on the Natural Terrain considering Geological Conditions, *The Journal of Engineering Geology*, **20(1),** 35-45 **(2010)**

16. Kim D., Im S., Lee S.H., Hong Y. and Cha K.S., Predicting the Rainfall-Triggered Landslides in a Forested Mountain Region Using TRIGRS Model, *J. Mt. Sci*., 7, 83–91 **(2010)**

17. Kim J., Choi C. and Park S., GIS-based landslide susceptibility analyses and cross-validation using a probabilistic model on two test areas in Korea, *Disaster Advances*, **6(10),** 45-54 **(2013)**

18. Kim K.S., Soil Characteristics according to the Geological Condition of Soil Slopes in Landslide Area, *The Journal of Engineering Geology*, **16(4),** 359-371 **(2006)**

19. Korean Geotechnical Society, Research contract report: addition and complement causes survey of Mt. Woomyeon landslide **(2011)**

20. Korean Society of Civil Engineers, Research contract report: causes survey and restoration work of Mt. Woomyeon landslide **(2012)**

21. Lambe T. W. and Whitman R. T., Soil mechanics, SI version, Wiley **(1979)**

22. Lee S., Choi J. and Min K., Landslide susceptibility analysis and verification using the Bayesian probability model, *Environmental Geology*, **43,** 120–131 **(2002)**

23. Lee S. and Choi U., Development of GIS-based geological hazard information system and its application for landslide analysis in Korea, *Geosciences Journal*, **7(3),** 243-252 **(2003)**

24. Lee S.W., Kim G., Yune C.Y. and Ryu H.J., Development of landslide-risk assessment model for mountainous regions in eastern Korea, *Disaster Advances*, **6(6),** 70-79 **(2013)**

25. Lee S. and Min K., Statistical analysis of landslide susceptibility at Yongin, Korea, *Environmental Geology*, **40,** 1095–1113 **(2001)**

26. Lee S., Ryu J.H. and Kim I.S., Landslide susceptibility analysis and its verification using likelihood ratio, logistic regression, and artificial neural network models, case study of Youngin, Korea, *Landslides*, **4,** 327-338 **(2007)**

27. Liu C.N. and Wu C.C., Mapping susceptibility of rainfall-triggered shallow landslides using a probabilistic approach, *Environ. Geol.*, **55,** 907-915 **(2008)**

28. Mathew J., Jha V.K. and Rawat G.S., Application of binary logistic regression analysis and its validation for landslide susceptibility mapping in part of Garhwal Himalaya, India, *International Journal of Remote Sensing*, **28(10),** 2257-2275 **(2007)**

29. Montrasio L., Valentino R. and Losi G.L., Towards a real-time susceptibility assessment of rainfall-induced shallow landslides on a regional scale, *Nat. Hazards Earth Syst. Sci*., **11,** 1927–1947 **(2011)**

30. Morrissey M.M., Wieczorek G.F. and Morgan B.A., A comparative analysis of hazard models for predicting debris flows in Madison County, Virginia. USGS **(2001)**

31. National Disaster Management Institute, A Study on Natural Landslide hazards Using Geographic Information Systems **(2003)**

32. National Forestry Cooperative Federation, Review report of restoration work of Mt. Woomyeon landslide **(2011)**

33. Nichol J. and Wong M.S., Satellite remote sensing for detailed landslide inventories using change detection and image fusion, *International Journal of Remote Sensing*, **26(9),** 1913-1926 **(2005)**

34. Safaei M., Omar H., Huat B.K., Yousof Z.B.M. and Ghiasi V., Deterministic rainfall induced landslide approaches, advantage and limitation, *Electronic journal of geotechnical engineering*, **16,** 1619-1650 **(2011)**

35. Saha A.K., Gupta R.P., Sarkar I., Arora M.K. and Csaplovics E., An approach for GIS-based statistical landslide susceptibility zonation-with a case study in the Himalayas, *Landslides*, **2,** 61-69 **(2005)**

36. Salciarini D., Godt J.W., Savage W.Z., Baum R.L. and Conversini P., Modeling landslide recurrence in Seattle, Washington, USA, *Eng. Geol*., **102,** 227-237 **(2008)**

37. Salciarini D., Godt J.W., Savage W.Z., Conversini P., Baum R.L. and Michael J.A., Modeling regional initiation of rainfall-induced shallow landslides in the eastern Umbria Region of central Italy, *Landslides*, **3,** 181–194 **(2006)**

38. Sidle R.C., Relative importance of factors influencing landsliding in coastal Alaska, 21st Annual Engng Geol. and Soils Engng Symp., 311-325 **(1984)**

39. Sorbino G., Sica C. and Cascini L., Susceptibility analysis of shallow landslides source areas using physically based models, *Nat. Hazards Earth Syst. Sci*., **53,** 313–332 **(2010)**

40. van Westen C.J., Geo-information tools for landslide risk assessment - an overview of recent developments, Proceedings of the 9th International Symposium on Landslides, Rio de Janeiro, 39-56 **(2004)**

41. van Westen C.J., Rengers N. and Soeters R., Use of geomorphological information in indirect landslide susceptibility assessment, *Natural Hazards*, **30,** 399–419 **(2003)**

42. van Westen C.J., Seijmonsbergen A.C. and Mantovani F., Comparing Landslide Hazard Maps, *Natural Hazards*, **20,** 137–158 **(1999)**

43. Varnes D.J., Slope movement types and process, National Academy of Science, Washington, D. C., special report, **2,** 11-33 **(1978)**

44. Vieira B.C., Fernandes N.F. and Filho O.A., Shallow landslide prediction in the Serra do Mar, Sao Paulo, Brazil, *Nat. Hazards Earth Syst. Sci.*, **10,** 1829–1837 **(2010)**

45. Yusof N., Ramli M.F., Pirasteh S. and Shafri H.Z.M., Landslides and lineament mapping along the Simpang Pulai to Kg Raja highway, Malaysia, *International Journal of Remote Sensing*, **32(14)** 4089-4105 **(2011)**

46. Zhou C.H., Lee C.F., Li J. and Xu Z.W., On the spatial relationship between landslides and causative factors on Lantau Island, Hong Kong, *Geomorphology*, **43,** 197-207 **(2002).**

Table 1
Dataset used in this study

Database	Format	GIS data type	Scale	Source
Hazard data	Landslide inventory	Point coverage	1:5,000	
Damageable objects	Buildings, roads, facilities	Line and polygon coverage	1:5,000	National Geographic Information Institute
Image data	Aerial photographs	GRID	25 × 25 cm	National Geographic Information Institute
	Satellite images	GRID	1 × 1 m	Commercial company
Hydrologic data	Precipitation	Point coverage	1:5,000	Korea Meteorological Administration
Basic data	Topographic map	Point and line coverage	1:5,000	National Geographic Information Institute
	Geotechnical investigation map	Point coverage	1:5,000	Field investigation reports
	Forest soil map	Polygon coverage	1:25,000	Korea Forest Service
	Geology map	Polygon coverage	1:50,000	Korea Institute of Geoscience And Mineral resources

.

Table 2
Summary of the field investigation and laboratory test values used in the simulations.

Parameter (unit)	**Zone 1**	**Zone 2**	**Zone 3**	**Zone 4**	**Zone 5**
Friction angle, ϕ (°)	25.3	28.5	37.6	30.9	28.2
Cohesion, c (kPa)	9.6	5.8	7.7	7.6	6.3
Total unit weight of soil, γ_s (KN/m^3)	18.1	17.7	17.0	17.3	18.2
Hydraulic conductivity of saturated, K_s (m/s)	7.15×10^{-6}	3.37×10^{-6}	1.80×10^{-6}	9.70×10^{-6}	3.69×10^{-6}
Saturated volumetric water content, θ_s	0.50	0.50	0.51	0.51	0.51
Residual volumetric water content, θ_r	0.20	0.20	0.19	0.19	0.19
Hydraulic diffusivity, D_0 (m^2/s)	200 K_s				
Steady infiltration rate, I_z (m/s)	0.01 K_s				

Table 3(a)
Soil strength according to soil texture.[31]

Parameter (unit)	**Sand (%)**	**Silt (%)**	**Clay (%)**	**Unit weight (KN/m^3)**	**Cohesion (kPa)**	**Internal friction angle (°)**
Silty clay loam	10	55	35	17.30	11.45	22
Silt loam	15	70	15	17.45	9.55	27
Sandy loam	70	15	15	19.10	4.05	28
Fine sandy loam	70	15	15	19.10	4.05	27
Clay loam	30	30	40	17.90	9.80	20
Loamy sand	80	10	10	19.40	2.70	30
Loamy fine sand	100	0	0	20.00	0.00	30
Loamy coarse sand	100	0	0	20.00	0.00	30
Loam	40	40	20	18.20	7.40	25

Table 3(b)
Soil properties according to soil texture.[7]

Soil texture	**b**	**ψ_s(cm)**	**θ_s**	**K_s (m/s)**
Sand	4.05	3.50	0.395	1.76×10^{-4}
Loamy sand	4.38	1.78	0.410	1.56×10^{-4}
Sandy loam	4.90	7.18	0.435	3.47×10^{-5}
Silt loam	5.30	56.60	0.485	7.20×10^{-6}
Loam	5.39	14.60	0.451	6.95×10^{-6}
Sandy clay loam	7.12	8.63	0.420	6.30×10^{-6}
Silty clay loam	7.75	14.60	0.477	1.70×10^{-6}
Clay loam	8.52	36.10	0.476	2.45×10^{-6}
Sandy clay	10.40	6.16	0.426	2.17×10^{-6}
Silty clay	10.40	17.40	0.492	1.03×10^{-6}
Clay	11.40	18.60	0.482	1.28×10^{-6}

Table 4(a)
Ranges and mean values for the cohesion and shearing resistance angle of soils according to the geological conditions.[18]

Geology	**Material**	**Cohesion (kPa)**			**Angle of shearing resistance (°)**		
		N	**Range**	**Mean**	**N**	**Range**	**Mean**
Gneiss	Landslide	28	1.6~29.6	8.8	28	18~38	33
	Non slide	27	1.1~10.6	5.1	27	31~39	36
	Total	55	1.1~29.6	7.1	55	18~39	34
Granite	Landslide	29	0.8~13.3	5.3	29	30~39	34
	Non slide	29	0.1~8.2	4.0	29	31~42	36
	Total	58	0.1~13.3	4.7	58	30~42	36
Sedimentary rocks	Landslide	39	1.5~8.5	4.5	39	31~37	34
	Non slide	42	0.7~12.0	4.8	42	31~41	36
	Total	81	0.7~12.0	4.6	81	31~41	36

Table 4(b)
Basic statistical analysis results of the major factors.[15]

Contents		**Coefficient of permeability (m/s)**		**Silt and clay contents (%)**		**Dry unit weight (KN/m^3)**	
		Non-occur.	**Occurrence**	**Non-occur.**	**Occurrence**	**Non-occur.**	**Occurrence**
Gneiss	N	513	45	500	28	513	45
	Mean	2.2E-3	2.4E-3	5.63	7.76	13.5	13.2
	Median	7.5E-5	7.6E-5	4.87	5.75	13.7	13.3
	Standard deviation	1.4E-3	9.6E-3	3.78	6.69	1.5	0.8
	Min. value	7.9E-7	3.0E-8	0.33	0.73	8.6	11.5
	Max. value	3.1E-2	6.3E-2	27.83	32.56	17.8	15.5
Granite	N	183	46	156	20	183	46
	Mean	2.0E-4	3.5E-5	5.45	13.39	12.9	13.1
	Median	1.0E-4	2.3E-6	4.67	7.70	13.0	13.3
	Standard deviation	2.4E-4	9.8E-5	4.53	11.52	1.7	1.4
	Min. value	6.3E-7	2.0E-8	0.37	2.78	9.9	10.3
	Max. value	9.8E-4	6.0E-4	28.51	40.46	17.2	15.8
Sedimentary rocks	N	36	-	36	-	36	-
	Mean	1.0E-4	-	10.32	-	12.7	-
	Median	3.7E-5	-	8.89	-	12.8	-
	Standard deviation	2.0E-4	-	6.16	-	1.5	-
	Min. value	1.0E-6	-	2.15	-	8.3	-
	Max. value	1.3E-3	-	21.80	-	15.9	-

Table 5
Summary of the cumulative frequency diagram for each class

Class (%)	Success rate		
	Geotechnical Investigation map	Soil texture map	Geology map
95 - 100%	72.4	25.5	20.0
90 - 100%	95.2	42.1	47.6
85 - 100%	97.9	52.4	64.8
80 - 100%	99.3	62.8	75.2
75 - 100%	100.0	73.8	84.8
70 - 100%	100.0	84.1	88.3
65 - 100%	100.0	88.3	93.1
60 - 100%	100.0	90.3	93.8
55 - 100%	100.0	93.8	95.2
50 - 100%	100.0	95.2	95.2
45 - 100%	100.0	95.9	95.2
40 - 100%	100.0	96.6	96.6
35 - 100%	100.0	96.6	97.9
30 - 100%	100.0	97.2	97.9
25 - 100%	100.0	98.6	99.3
20 - 100%	100.0	99.3	99.3
15 - 100%	100.0	99.3	100.0
10 - 100%	100.0	100.0	100.0
5 - 100%	100.0	100.0	100.0
0 - 100%	100.0	100.0	100.0

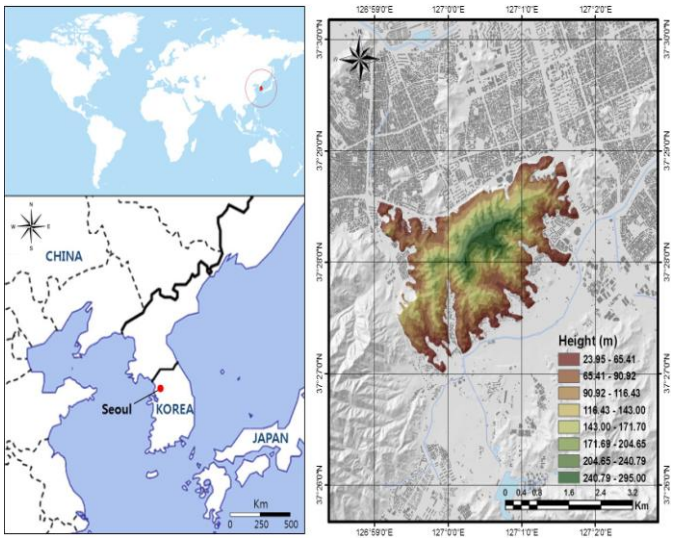

Fig. 1: Location map of the Woomyeon Mountain region in Seoul, South Korea.

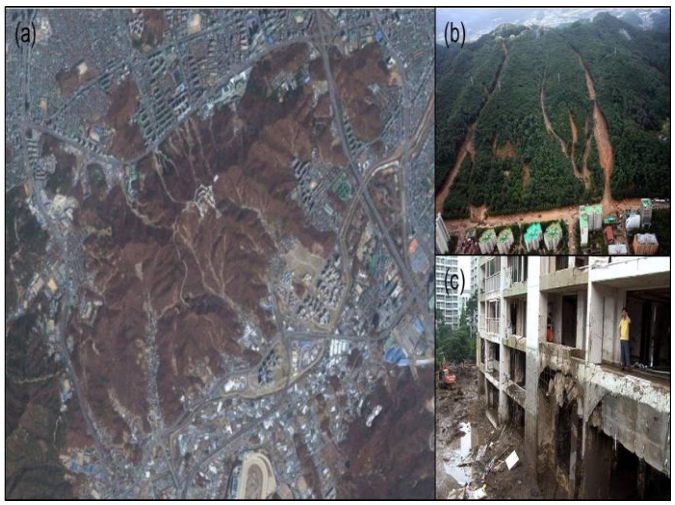

Fig. 2: Overview of the Woomyeon Mountain landslide event on 27 July 2011:
(a) landslides and debris flow scarps, (b) debris flow hazards and (c) damaged apartments.

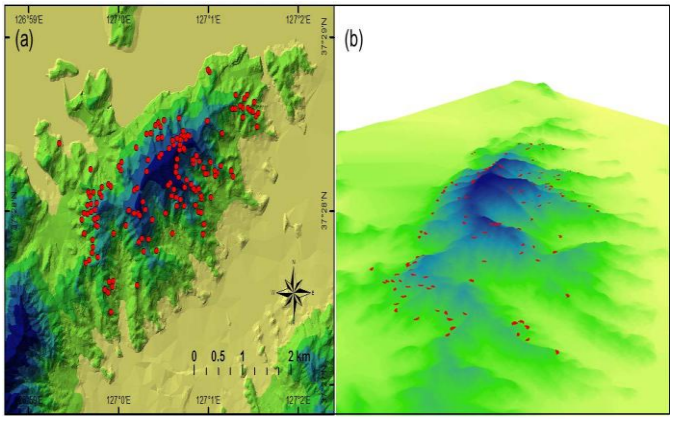

Fig. 3: Landslide inventory map of the study area: (a) landslides scars mapping and (b) three-dimensional plot of the landslides.

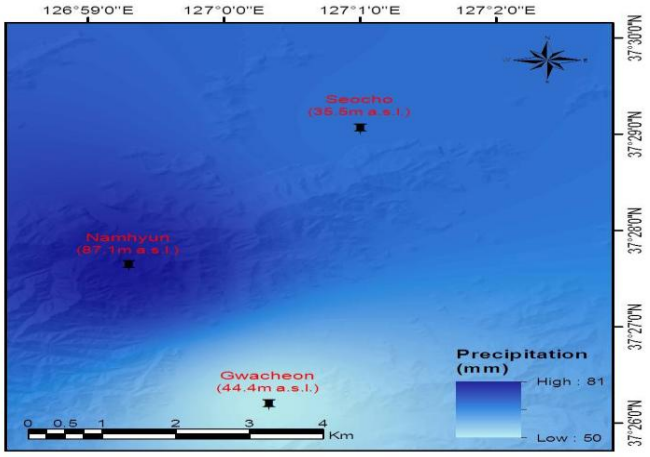

Fig. 4: Section of the rainfall input layers (hourly rainfall intensity from 08:00 to 09:00 on 27 July 2011).

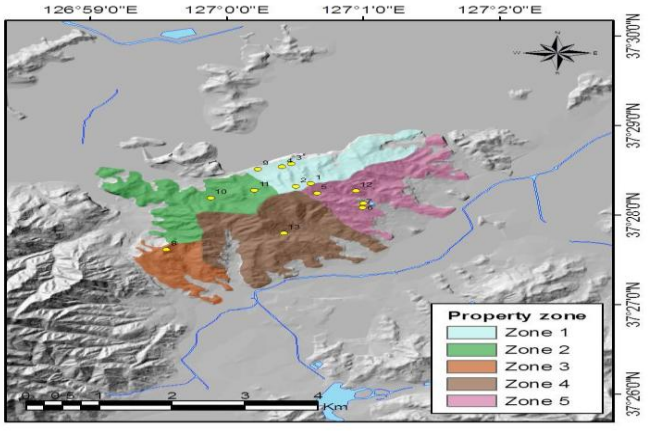

Fig. 5: Locations of the investigation boreholes for sampling soils and the map showing the property zones. The soil parameters for each zone are detailed in table 2.

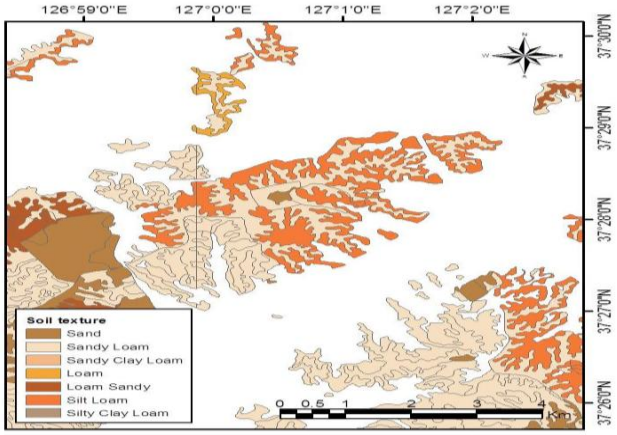

Fig. 6: Soil texture map of the study area: the soil parameters for each texture are detailed in tables 3(a) and 3(b).

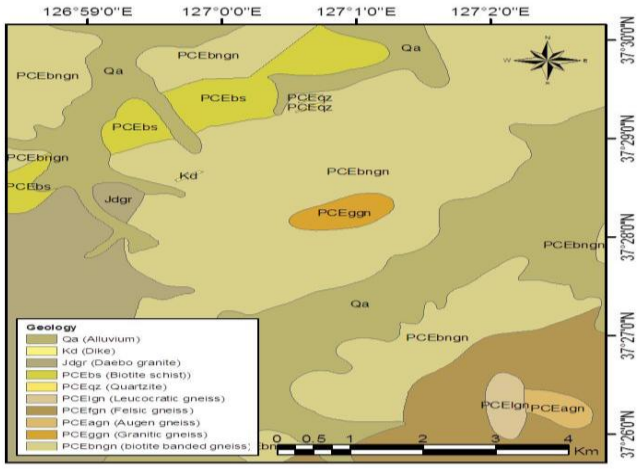

Fig. 7: Geological map of the study area: the soil parameters for each geology are detailed in tables 4(a) and 4(b).

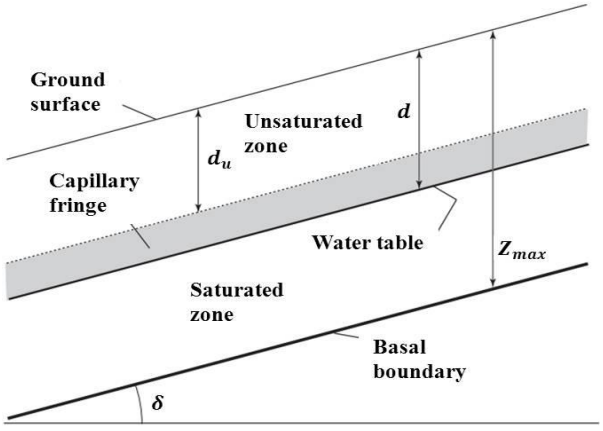

Fig. 8: Conceptual diagram of the TRIGRS model.

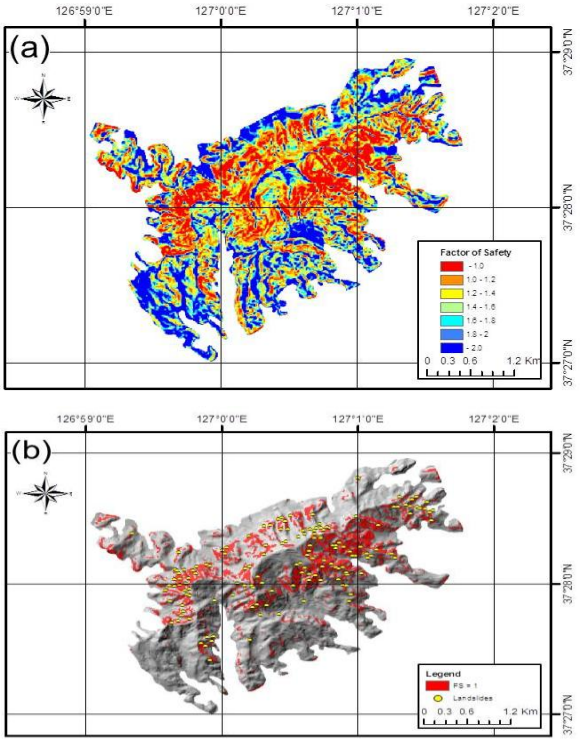

Fig. 9: Spatial distributions of the simulation results using the geotechnical investigation database: (a) resulting map of safety factors and (b) resulting map of unstable areas (FS< 1).

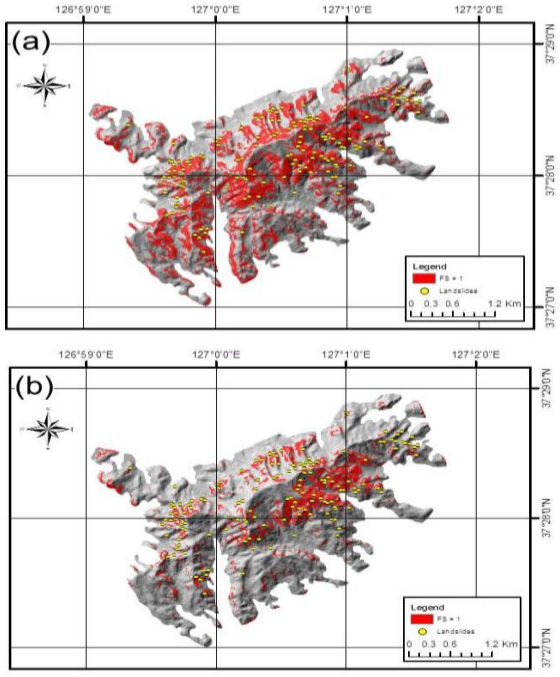

Fig. 10: Spatial distribution of the unstable area (FS < 1) according to TRIGRS in the study area: simulation results using (a) the soil texture database and (b) the geology database.

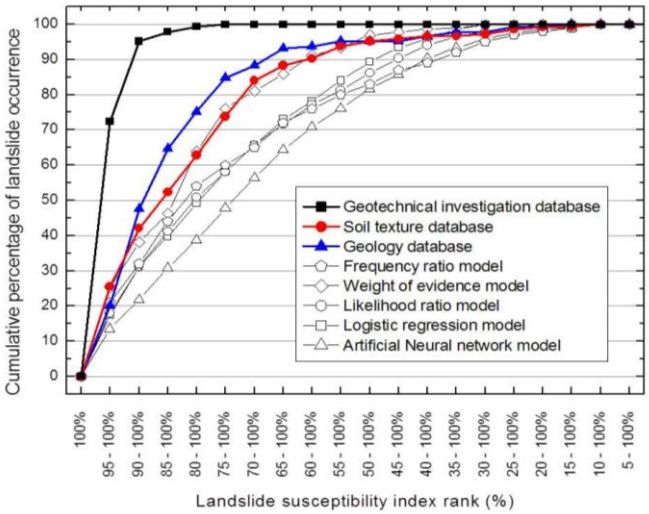

Fig. 11: Cumulative frequency diagram showing the landslide susceptibility index rank occurring in the cumulative percentage of landslide occurrence.

(Received 11th November 2013, accepted 29th December 2013)